Supplementary Information

Multi-model evidence of future tropical Atlantic precipitation change modulated by AMOC decline

Authors:

Giada Cerato[1*], Katinka Bellomo[1,2], Roberta D'Agostino[3], and Jost von Hardenberg[1,2]

Affiliations:

[1]Polytechnic University of Turin, Department of Environment, Land, and Infrastructure Engineering, Turin, Italy

[2] National Research Council, Institute of Atmospheric Sciences and Climate, Turin, Italy

[3] National Research Council, Institute of Atmospheric Sciences and Climate, Lecce, Italy

Table S1: List of models: model's name, variant label (ensemble member), AMOC change (in Sv and percentage) computed as the difference between years 2071-2100 and 1850-2014, and AMOC historical mean strength averaged over years 1850-2014.

Model	Variant label	ΔAMOC [Sv]	ΔAMOC [%]	AMOC mean strength [Sv]
ACCESS-CM2	r1i1p1f1	-7.23	-39.25	18.43
ACCESS-ESM1-5	r1i1p1f1	-5.21	-28.79	18.09
CanESM5	r1i1p1f1	-5.67	-45.56	12.46
CanESM5-CanOE	r1i1p2f1	-5.45	-44.44	12.26
CAS-ESM2-0	r1i1p1f1	-5.82	-30.11	19.33
CESM2	r10i1p1f1	-10.32	-55.15	18.72
CESM2-WACCM	r1i1p1f1	-9.80	-53.21	18.42
CMCC-CM2-SR5	r1i1p1f1	-6.36	-36.47	17.44
CMCC-ESM2	r1i1p1f1	-6.73	-38.3	17.57
CNRM-CM6-1	r1i1p1f2	-7.87	-48.13	16.35
CNRM-CM6-1-HR	r1i1p1f2	-6.86	-49.23	13.93
CNRM-ESM2-1	r1i1p1f2	-7.54	-45.03	16.74
FGOALS-f3-L	r1i1p1f1	-4.34	-21.94	19.78
FGOALS-g3	r1i1p1f1	-10.60	-37.75	28.07
GFDL-CM4	r1i1p1f1	-8.40	-45.85	18.32
GFDL-ESM4	r1i1p1f1	-8.55	-45.96	18.61
GISS-E2-1-G	r1i1p1f2	-13.44	-55.24	24.33
GISS-E2-2-G	r1i1p3f1	-10.74	-43.71	24.57
HadGEM3-GC31-LL	r1i1p1f3	-6.545	-39.79	16.44
HadGEM3-GC31-MM	r1i1p1f3	-8.534	-49.75	17.15
INM-CM4-8	r1i1p1f1	-6.197	-31.22	19.84
INM-CM5-0	r1i1p1f1	-5.11	-25.97	19.69
MIROC6	r1i1p1f1	-6.07	-42.94	14.14
MIROC-ES2L	r1i1p1f2	-5.563	-44.52	12.49
MPI-ESM1-2-HR	r1i1p1f1	-5.458	-32.15	16.97
MPI-ESM1-2-LR	r1i1p1f1	-4.651	-24.73	18.80
MRI-ESM2-0	r1i1p1f1	-11.587	-62.82	18.44
NorESM2-LM	r1i1p1f1	-12.15	-57.98	20.96
NorESM2-MM	r1i1p1f1	-12.12	-56.34	21.51
UKESM1-0-LL	r1i1p1f2	-6.184	-40.10	15.42

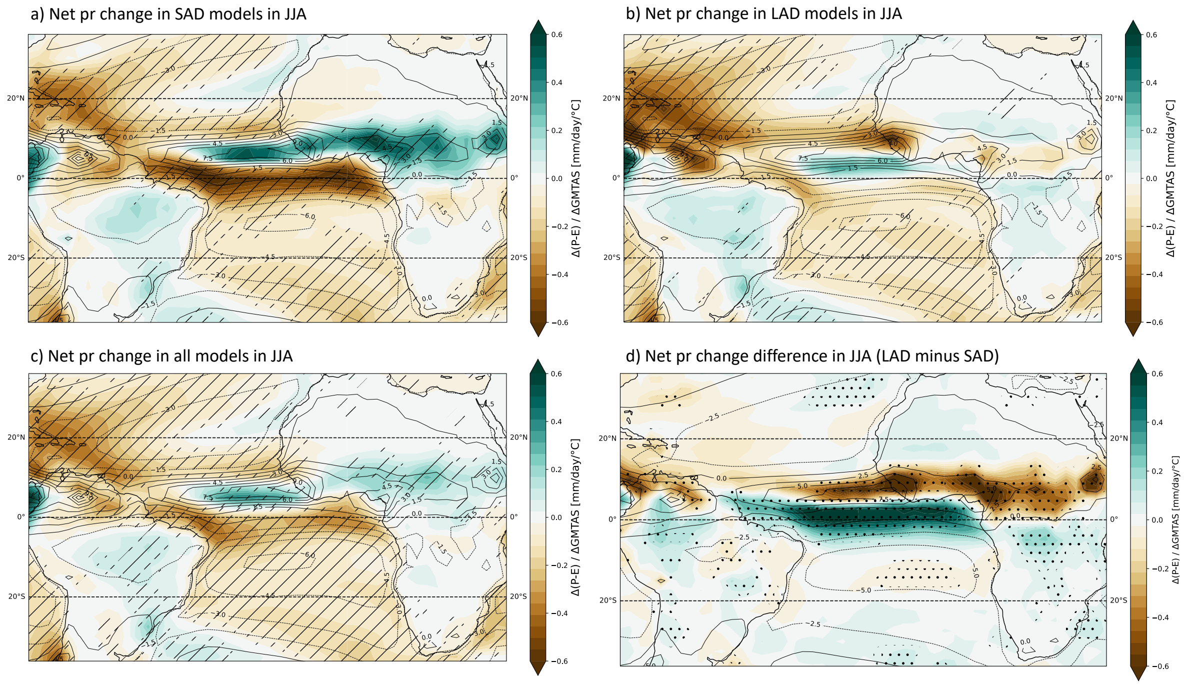

Figure S1: Net precipitation (P-E) change in JJA. Panels a, b and c display the normalized annual mean net precipitation change between the historical simulation (years 1850 through 2014) and years 2071 through 2100 of the ssp585 simulation in JJA season for the SAD group, the LAD group, and all the models, respectively. Superimposed contours show the mean annual net precipitation climatology in JJA computed as the ensemble mean of the historical run of all models. Hatches indicate where the statistical t-test between the historical and future net precipitation change is statistically significant at the 90% level of a Student's t-test. Panel d shows the difference between the LAD and the SAD net precipitation change (Panel b minus Panel a). Stippling indicates where net precipitation change differences between the LAD and SAD ensemble means are statistically relevant at the 90% level of a Student's t-test.

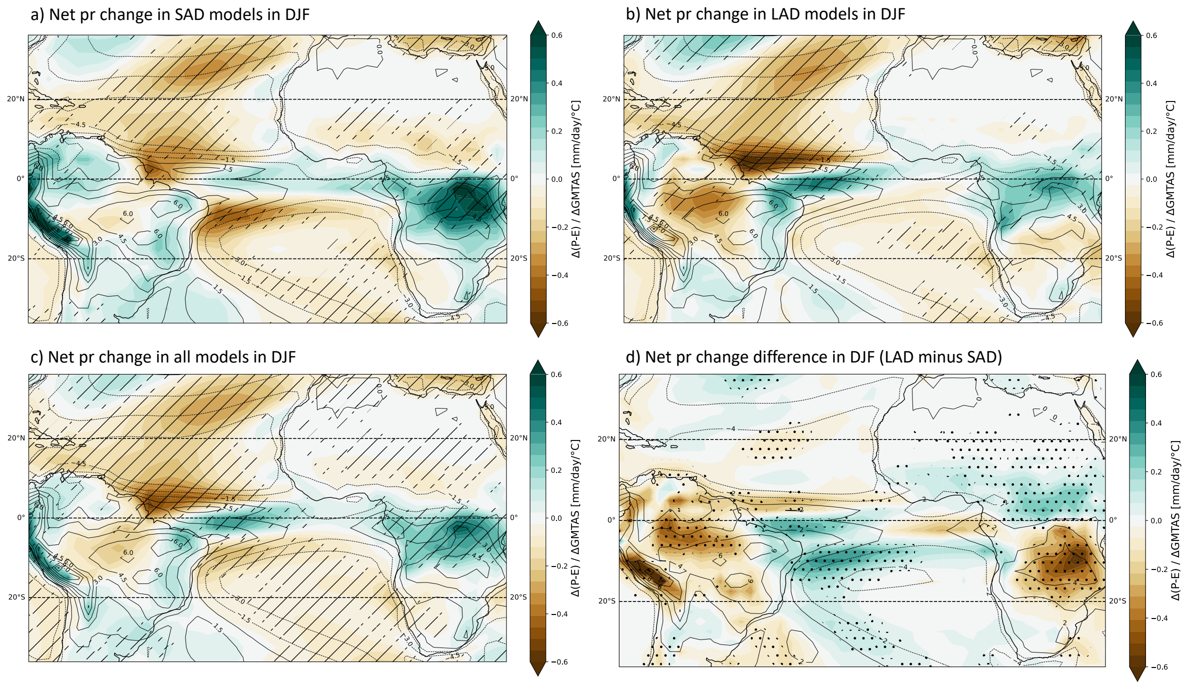

Figure S2: Net precipitation (P-E) change in DJF. Panels a, b and c display the normalized annual mean net precipitation change between the historical simulation (years 1850 through 2014) and years 2071 through 2100 of the ssp585 simulation in DJF season for the SAD group, the LAD group, and all the models, respectively. Superimposed contours show the mean annual net precipitation climatology in DJF computed as the ensemble mean of the historical run of all models. Hatches indicate where the statistical t-test between the historical and future net precipitation change is statistically significant at the 90% level of a Student's t-test. Panel d shows the difference between the LAD and the SAD net precipitation change (Panel b minus Panel a). Stippling indicates where net precipitation change differences between the LAD and SAD ensemble means are statistically relevant at the 90% level of a Student's t-test.

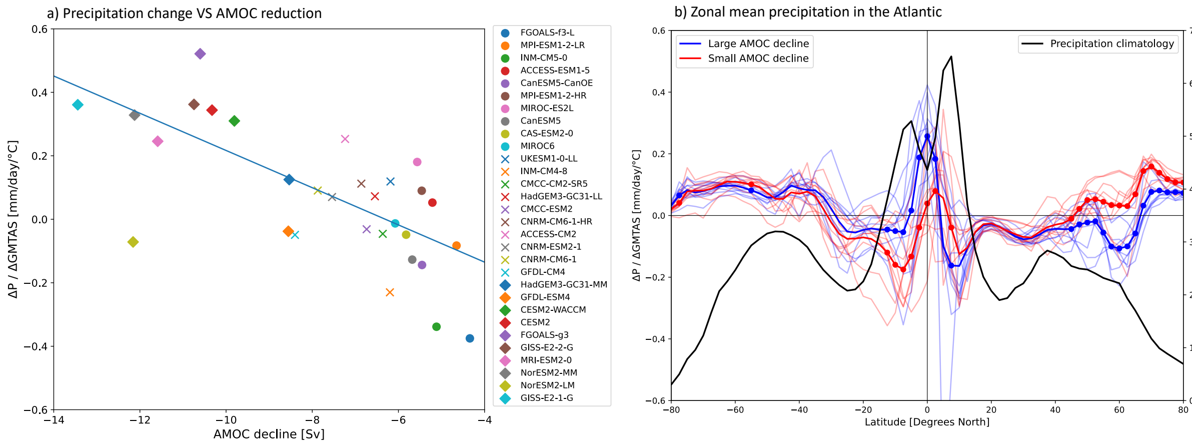

Figure S3: Meridional displacement of tropical Atlantic precipitation. Panel a shows the normalized precipitation change difference between the two boxes in Figure 1c (south box minus north box), against the AMOC reduction expressed in Sv. Circles indicate the SAD models, diamonds indicate the LAD models, and crosses indicate the other models in between. The blue line is the robust Huber regression ($y = -0.37 - 0.06x$), with $R^2 = 0.46$. Panel b displays the zonal mean annual mean precipitation in the Atlantic sector (between 60 °W and 10 °E): the black curve shows the climatological precipitation computed from all the historical simulations (years 1850 through 2014); the red curves show net precipitation change for the members of the SAD group and the SAD group ensemble mean (thicker red curve); the blue curves show net precipitation change for the members of the LAD group and the LAD group ensemble mean (thicker blue curve). Markers (filled circles) on the curves indicate where the differences between the SAD and LAD groups are significant at 90% level of a Student's t-test.

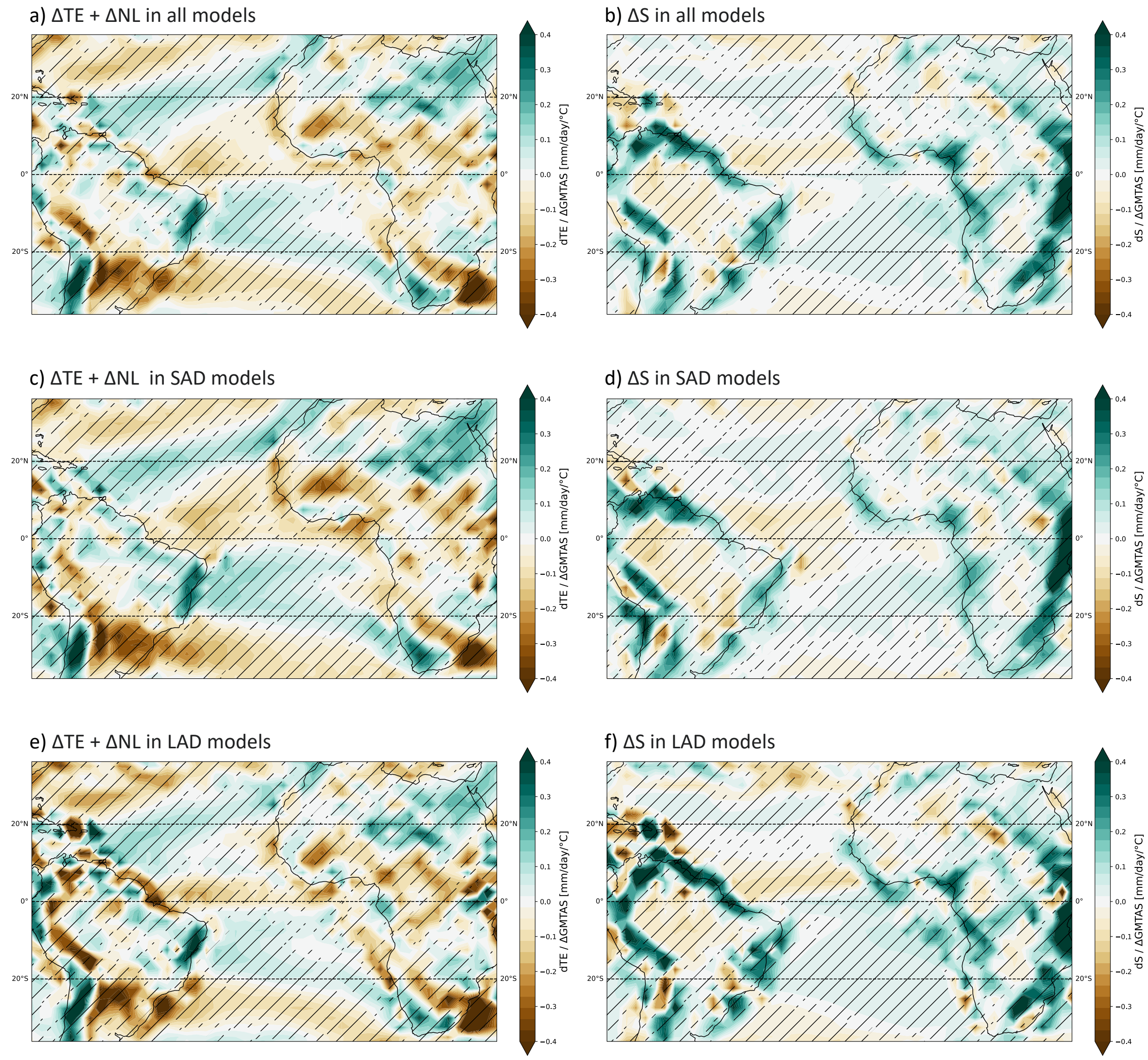

Figure S4: Terms ΔTE + ΔNL and ΔS of the moisture budget. Panels a, c and e show changes in the transient eddies + nonlinear terms contribution $(\Delta TE + \Delta NL)$ to the moisture budget for the SAD group, the LAD group, and all models, respectively, computed as described in the text. Panels b, d and f show changes in the surface quantities contribution (ΔS) to the moisture budget for the SAD group, the LAD group, and all models, respectively. Hatches are localized where at least two-thirds of the models agree in the sign of change.

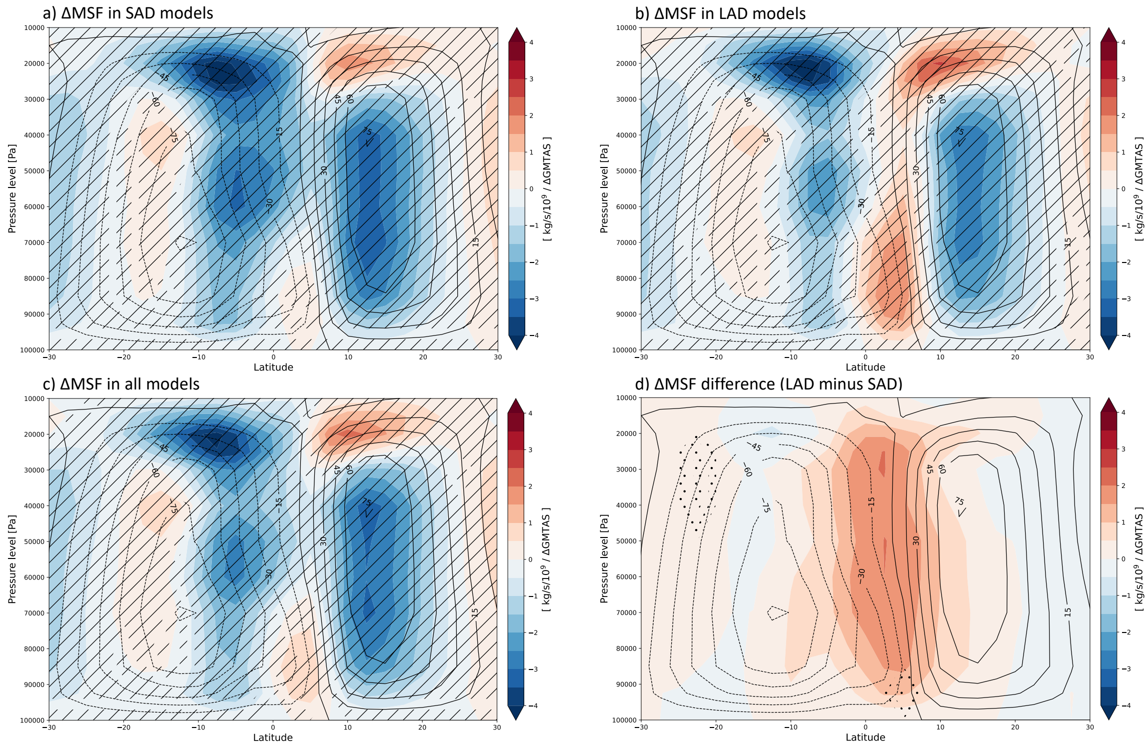

Figure S5: Global atmospheric circulation changes. Panels a, b and c display the normalized global annual mean atmospheric circulation change between the historical simulation (years 1850 through 2014) and years 2071 through 2100 of the ssp5-8.5 simulation for the SAD group, the LAD group, and all models, respectively. Superimposed contours show the mean annual atmospheric circulation climatology computed as the ensemble mean of the historical run of all models. Hatches indicate where the statistical t-test between the control and future net precipitation distribution is statistically significant at the 90% level. Panel d represents the difference between the LAD and the SAD atmospheric circulation anomalies (Panel b minus Panel a). Stippling indicates where atmospheric circulation change differences between the LAD and SAD ensemble means are statistically significant at the 90% level of a Student’s t-test.

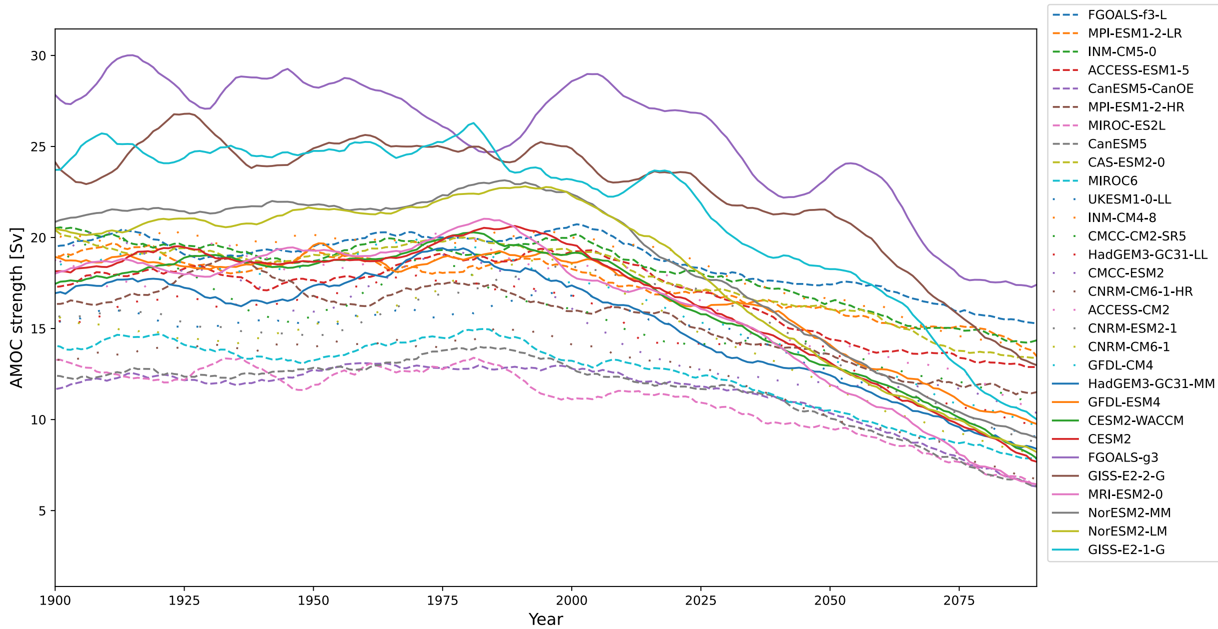

Figure S6: Annual mean AMOC strength index between years 1900 and 2090 (absolute values). A 15-year running mean has been applied. Dashed lines represent models in the SAD group, solid lines represent models in the LAD group, dotted lines represent other models in between.

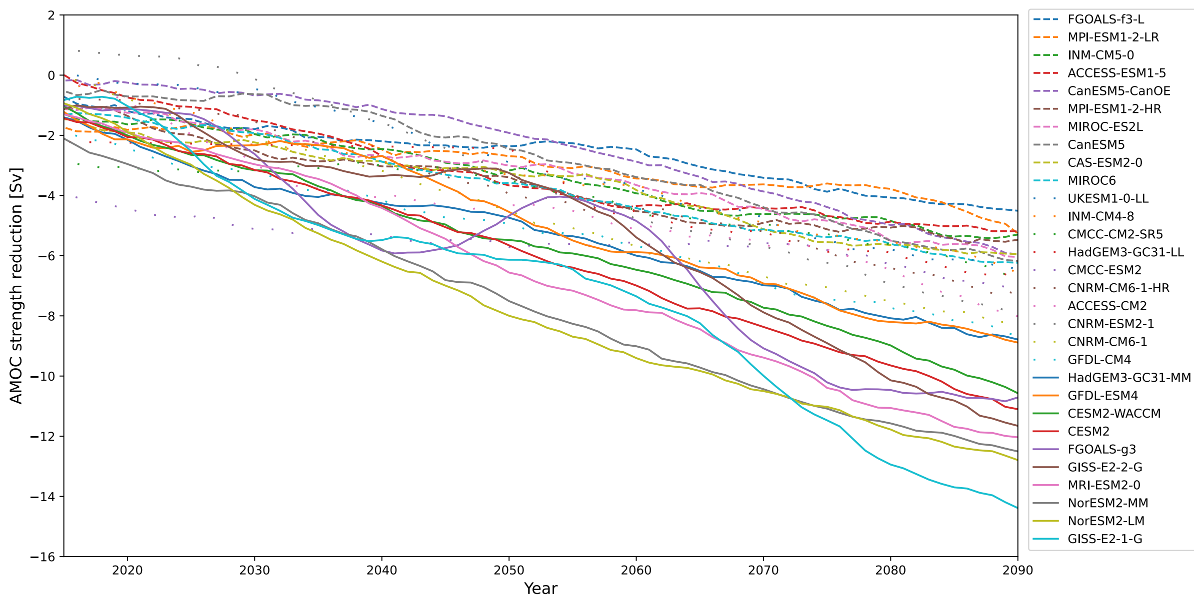

Figure S7: Annual mean AMOC strength index change with respect to the mean historical value (see Table S1). A 15-year running mean has been applied. Dashed lines represent models in the SAD group, solid lines represent models in the LAD group, dotted lines represent other models in between.

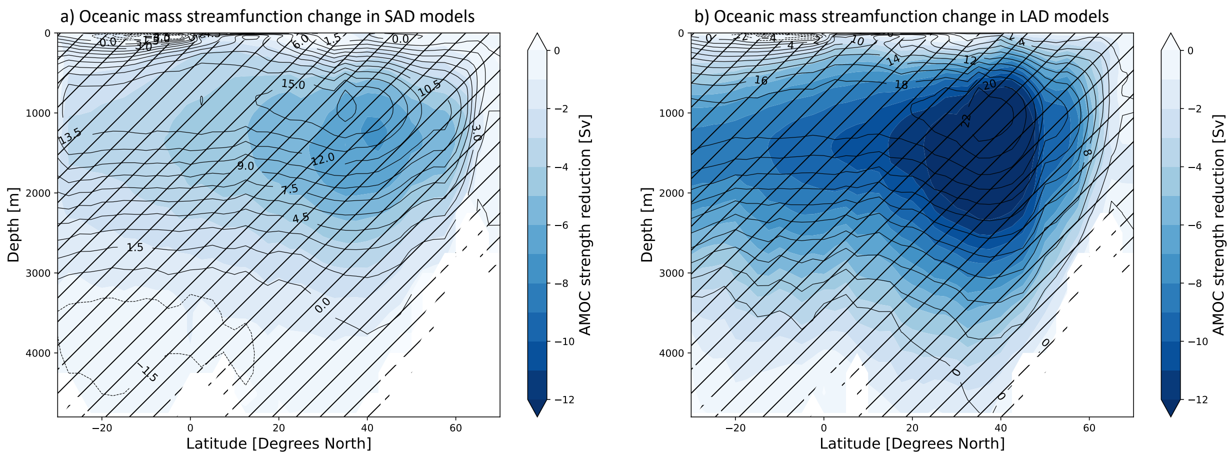

Figure S8: **Oceanic mass streamfunction change.** Panels a and b show a transect of the Atlantic ocean and display the overturning mass streamfunction change between the historical simulation (years 1850 through 2014) and years 2071 through 2100 of the ssp5-8.5 simulation for the SAD group and the LAD group, respectively. Black contours represent the respective climatology for the two groups of models computed separately as the ensemble mean of the historical run of two groups models. Hatches indicate where the statistical t-test between the control and future mass streamfunction is statistically significant at the 90% level.